Assimilation of Mode-S observations in ALADIN/CHMI

Alena Trojáková, Patrik Benáček, Radmila Brožková a Antonín Bučánek

Contents

1 Assimilation of aircraft Mode-S observations in ALADIN/CHMI

Modern air traffic surveillance systems have received substantial attention in recent years due to its capability to provide not only an accurate knowledge of the position of the aircraft, but also meteorological information (de Haan, 2011; Strajnar, 2012). The secondary radars operating in the S mode (Mode-S) communicating with an active transponder-equipped aircraft can determine the mandatory Mode-S Enhanced Surveillance (EHS) parameters and optional parameters from the special Mode-S Meteorological Routine Air Report (MRAR) register. Mode-S EHS data contain indirect meteorological information, while Mode-S MRAR data provides direct observation of both air temperature and wind.

This study aims to explore a potential of new Mode-S aircraft observations to improve the short-range numerical weather forecast. The state-of-the-art NWP system ALADIN/CHMI and aircraft observations used in this study are briefly described. The quality of Mode-S data available in the airspace of the Czech Republic is evaluated. Finally, first results of assimilation studies evaluating an impact of the Mode-S MRAR observations are discussed.

1.1 NWP system ALADIN/CHMI

A general meso-scale forecasting tool ALADIN has been developed in an international collaboration since 1991, taking the ARPEGE/IFS global model as a backbone. ALADIN version used in this study is based on the operational setting at Czech Hydrometeorological Institute (ALADIN/CHMI), covering computational domain of Central Europe, with horizontal mesh size of 4.7 km, 87 vertical levels and time-step of 180 s.

ALADIN/CHMI couples hydrostatic dynamics and the set of ALARO-1 physical parametrizations suited for modeling atmospheric motions from planetary up to the meso-gamma scales. Surface processes are parametrized by the land surface scheme Interaction Soil Biosphere Atmosphere (ISBA) (Noilhan and Planton, 1989; Giard and Bazile, 2000). The soil moisture, together with snow depth, vegetation and other parameters, is very important component of the surface water and energy budgets. Following Giard and Bazile (2000), the assimilation of screen-level observations using optimal interpolation (OI) is used to provide an analysis of the soil prognostic variables. The upper-air initial conditions are provided by the BlendVar scheme which combines Digital Filter (DF) Blending method (Brožková *et al.*, 2001) with the 3D-Var method. The variational code of the ALADIN 3D-Var is based on the incremental formulation originally introduced in the ARPEGE/IFS global assimilation (Courtier *et al.*, 1994). The control vector is composed of vorticity, divergence, temperature, specific humidity and surface pressure. Prognostic water species and other convection and turbulence related variables are used from the background. The specification of the background error covariance matrix follows Berre (2000).

The BlendVar scheme uses a six-hour forward intermittent cycle, see Figure 1. A six-hour forecast from a previous cycle is used as the first guess or background. First the surface analysis updates the soil prognostic variables (temperature and water content) by optimal interpolation of screen-level observations, while sea temperatures are taken from the global ARPEGE analysis. Then upper-air prognostic variables are blended with the global ARPEGE analysis using the DF Blending scheme. Afterwards the 3D-Var assimilation combines the blended background and available observations by minimizing the cost function:

$$J(\boldsymbol{x}) = \frac{1}{2}(\boldsymbol{x} - \boldsymbol{x}_b)^T \boldsymbol{B}^{-1}(\boldsymbol{x} - \boldsymbol{x}_b) + \frac{1}{2}(\boldsymbol{y} - H(\boldsymbol{x}))^T \boldsymbol{R}^{-1}(\boldsymbol{y} - H(\boldsymbol{x})), \tag{1}$$

where $\boldsymbol{x}$ is an analyzed model state vector, $\boldsymbol{x}_b$ is the blended background, $\boldsymbol{y}$ is a vector of observations, H is generally a non-linear observation operator, $\boldsymbol{R}$ is an observation error covariance matrix and $\boldsymbol{B}$ is a background error covariance matrix. The analysis is used as initial condition for the subsequent

six-hour forecast to create the first guess of the next assimilation cycle. The assimilation system is applied with 6-hour cycling at 00, 06, 12 and 18 UTC. The BlendVar assimilates most of conventional observations and satellite radiances from Spinning Enhanced Visible and Infrared Imager (SEVIRI) on board of geostationary satellite Meteosat-10. The assimilated conventional observations comprise air pressure from surface synoptic stations (SYNOP), temperature, humidity and wind measurements from aerological soundings (TEMP), temperature and wind observation from aircraft (AMDAR) and atmospheric motion vectors (AMV) derived from Meteosat-10. Only aircraft data are analyzed within a 3-hour assimilation window, all other observations are assimilated only at analysis time.
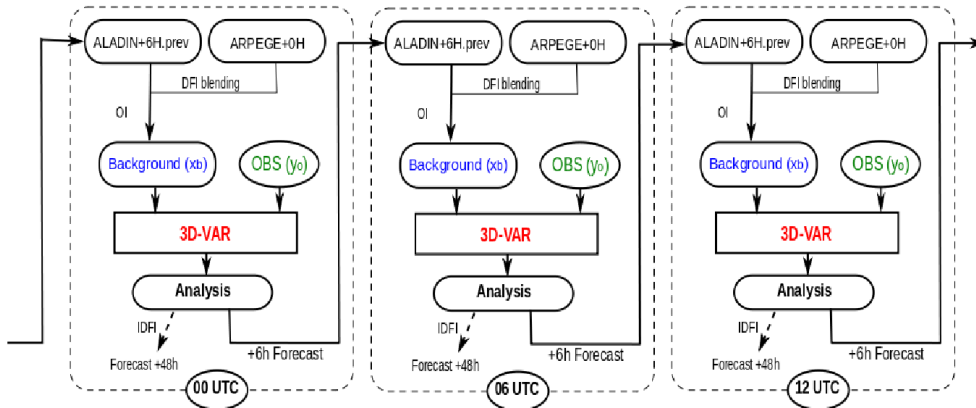
Figure 1: The BlendVar assimilation scheme.

1.2 Aircraft observations

Aircraft-based observations are one of the key components of the Global Observing System and the World Weather Watch Programme of the World Meteorological Orgnisation (WMO). The automated collection and transmition of meteorological observations from aircraft is well established and provides support to the upper-air monitoring of the atmosphere and meteorological applications. The main source of aircraft-based observation is derived from the Aircraft Meteorological DAta Relay (AMDAR) system (Painting, 2003). Novel approaches using enhanced surveillance air traffic control radar have been exploited only recently. They are considered very interesting and potentially very helpful for regional modeling and nowcasting applications.

1.2.1 AMDAR

AMDAR system facilitates the fully automated collection and transmission of weather observations from commercial aircraft. The system is operated by WMO Member National Meteorological and Hydrological Service in cooperation with partner airlines. The AMDAR program is currently served by a worldwide fleet of over 3000 aircraft contributing more than 400000 high quality upper air observations per day (WMO, 2014a). Studies and experiments have shown that AMDAR and other aircraft-based observations generally provide an improvement in forecasting ability through a reduction in NWP forecast error of up to 20% (WMO, 2014b).

AMDAR collects and distributes meteorological variables (air temperature, wind speed and direction), accurate measurements of time and position (latitude, longitude and pressure altitude), measurements of turbulence and water vapor or humidity data, if the aircraft is appropriately equipped. A typical reporting frequency while aircraft is on ascent/descent is in lower troposphere by 10 hPa intervals (or 6/60 second intervals), in the middle to the upper troposphere by 50 hPa intervals (or

20/60 second intervals), while reporting en route is in 3 to 7-minute intervals. The uncertainty of AMDAR measurements is estimated around 0.4°C for temperature and and 2–3 m/s for wind, more details can be found in Painting (2003).

1.2.2 Mode-S

The secondary radars operating in the S mode (Mode-S) can determine the mandatory Mode-S Enhanced Surveillance (EHS) parameters and optional parameters from the special Mode-S Meteorological Routine Air Report (MRAR) register. Mode-S EHS data contain indirect meteorological information (de Haan, 2011), while Mode-S MRAR data provides direct observation of both air temperature and wind (Strajnar, 2012).

This section presents an overview of Mode-S data provided by Air Navigation Services of the Czech Republic (ANS CR) in the scope of the project. In the Czech Republic, there are three Mode-S radars located at Prague and on the Pisek and Buchtuv kopec hills. We also receive data from Germany, Slovakia and the most recently from Austria, see Table 1. The research Mode-S data sample contains parameters specified in Table 2.

Name	Latitude [deg]	Longitude [deg]	Range [km]	Mode-S data
PRAHA	50.086 N	14.270 E	296	MRAR,EHS
BUKOP	49.660 N	16.133 E	370	MRAR,EHS
PISEK	49.786 N	14.035 E	296	EHS
JAVOR	48.261 N	17.163 E	296	EHS
AUERSBG	50.456 N	12.648 E	278	EHS
VIENNA	48.102 N	16.578 E	222	EHS

Table 1: Overview of available radars.

Source	Parameter	Unit
EHS	ICAO address	
EHS	lat/lon	[deg]
EHS	flight level	[100 feet]
EHS	ground speed	[m/s]
EHS	true air speed	[m/s]
EHS	Mach number	[1]
EHS	heading angle	[deg]
EHS	roll angle	[deg]
MRAR	air temperature	[K]
MRAR	air wind speed	[m/s]
MRAR	air wind direction	[deg]

Table 2: Overview of available Mode-S EHS and MRAR parameters.

Available Mode-S data between 1 July and 31 October 2015 were analyzed (with a gap between 19 and 30 October due to technical problems with the data provision). The Mode-S EHS comprise around 3.5 million of measurements per day and from that 85% is above 6000 meters. The Mode-S MRAR are much less frequent and involve only around 140000 per day (66% above 6000 meters). A typical reporting frequency is 10 s. The coverage of Mode-S data is illustrated in Figure 2. The

diurnal cycle of the data availability follows air traffic over the Czech Republic with a broad peak around noon and a very limited number of data at night.
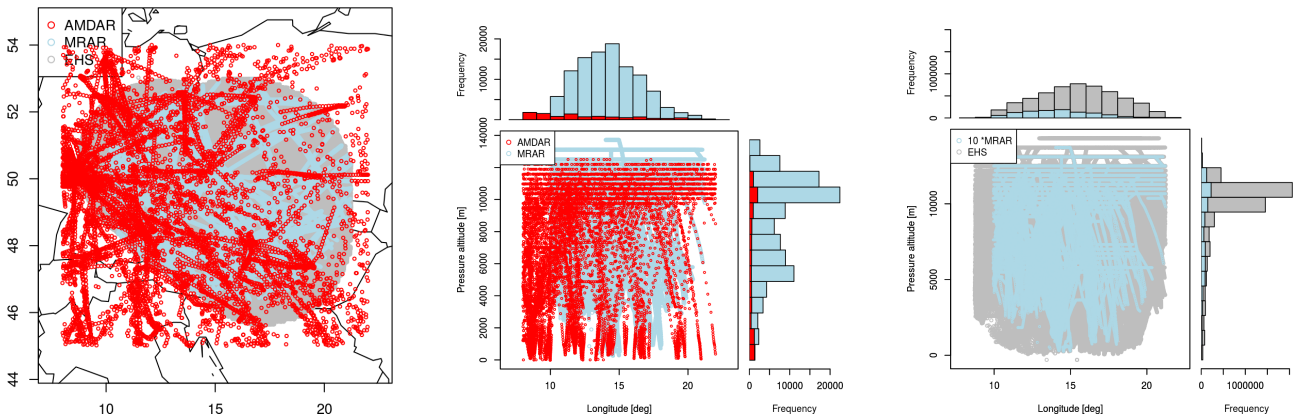
Figure 2: Horizontal (left) and vertical (middle, right) coverage of Mode-S EHS/MRAR and AMDAR data on 1 August 2015.

Aircraft type identification

Mode-S equipment on aircraft are assigned by a unique ICAO 24-bit address (ICAO address). The ICAO address is assigned by flight authorities in each country and provides an unique identification of a meteorological sensor of each aircraft. Although no centralized aircraft database is available publicly, it is possible to relate ICAO address with aircraft type information either using online sources (various flight tracking and/or place spotter websites) or using flight plans available to ANS CR. In this study only the first approach is considered, but in the future a combination of both will be used to identify as many aircraft as possible. The Mode-S data contain around 13000 different aircraft and around 2300 remained unidentified. Table 3 shows the number of aircraft from the most represented aircraft types.

Type	Number of aircraft	Type	Number of aircraft
Airbus A319	586	Bombardier Global 5000	69
Airbus A320	1170	Bombardier Global 6000	122
Airbus A321	460	Canadair CL604 Challenger	74
Airbus A330	538	Canadair CL605 Challenger	65
Airbus A340	146	Canadair CRJ	125
Airbus A380	173	Cessna 510 Citation Mustang	66
ATR 72	52	Cessna 560XLS Citation Excel	55
Boeing 737	1676	Dassault Falcon 2000EX	57
Boeing 747	405	Dassault Falcon 7X	110
Boeing 757	159	Embraer ERJ	293
Boeing 767	358	Gulfstream G450	63
Boeing 777	906	Gulfstream G550	70
Boeing 787	182	McDonnell Douglas MD	98
Bombardier Dash 8 Q400	98	unknown	2303

Table 3: Number of aircraft from different aircraft types (only types with more than 50 aircraft are listed).

1.3 Validation of Mode-S observation observations

Any measurement is prone to error, which depends on an instrumental accuracy and a methodology. The accuracy of a new meteorological observation is widely assessed by comparison with other measurements or with a NWP model (de Haan, 2011). Such a comparison provides only indirect error estimation, since it combines errors of both the new and the reference data. An independent measurement technique can be used to address systematic errors, e.g. a comparison of aircraft and radiosonde measurement, (Schwartz and Benjamin, 1995). For an estimation of the standard deviation of observation errors even the same method using an independent instrument can be used, e.g. a comparison of temperature measurement from different aircraft, (Benjamin *et al.*, 1999).

Following studies of de Haan (2011) and Strajnar (2012) a collocation technique with respect to AMDAR data and NWP model ALADIN/CHMI is used to validate available Mode-S data over period of 1 July – 20 October 2015.

1.3.1 Mode-S and AMDAR collocation

Although both AMDAR and Mode-S belong to the same group of aircraft observation and AMDAR and Mode-S MRAR temperature even originate from the same sensor, they differ due to a preprocessing or the reporting frequency. The AMDAR preprocessing, which comprises smoothing and averaging, precludes the absolute space and time match of AMDAR and Mode-S data. To find Mode-S and AMDAR observation pairs, so called collocated observations, a predefined time mismatch and space separation are allowed, see Table 4. When more possible pairs are found within defined criteria the closest in the space is selected. There were found around 21000 MRAR - AMDAR pairs and around 384000 EHS - AMDAR pairs during the studied period from July till October 2015. Figure 3 shows distributions of the collocated pairs.

Parameter	separation
time difference	30 s
height difference	50 m
horizontal distance	15 km

Table 4: Time mismatch and space separation of collocated Mode-S and AMDAR pairs
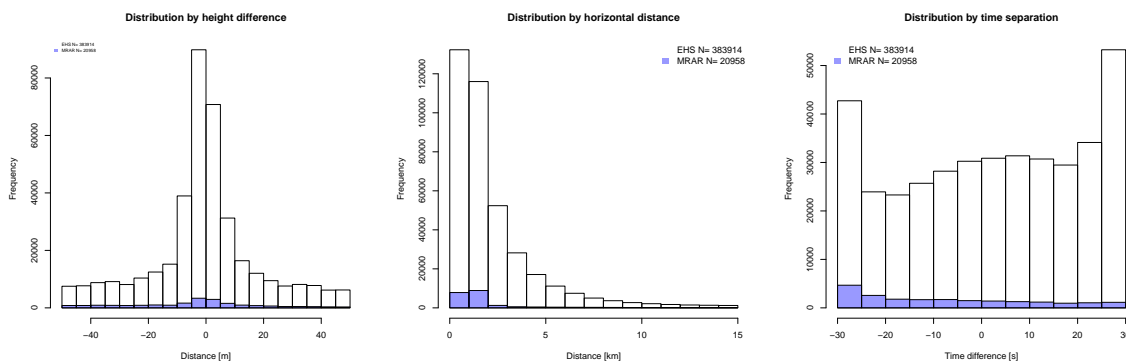
Figure 3: Distribution of Mode-S EHS/MRAR and AMDAR matches by height difference (left), horizontal (middle) and time (left) separation.

Differences between Mode-S MRAR and AMDAR contain a small number of outliers, e.g. the single erroneous AMDAR wind speed value of 361 m/s and several non-representative temperature values close to the Prague airport, probably affected by local conditions on runway prior to takeoff or

after landing. The outliers (differences larger than 4 K, 10 m/s and 50°) were excluded from the data analysis, e.g. histogram computations displayed in Figure 4, but the basic statistics for the complete data set are indicated in the plots as well. Differences are mostly normally distributed and have small spread, which means a good agreement of Mode-S MRAR data with AMDAR observations.
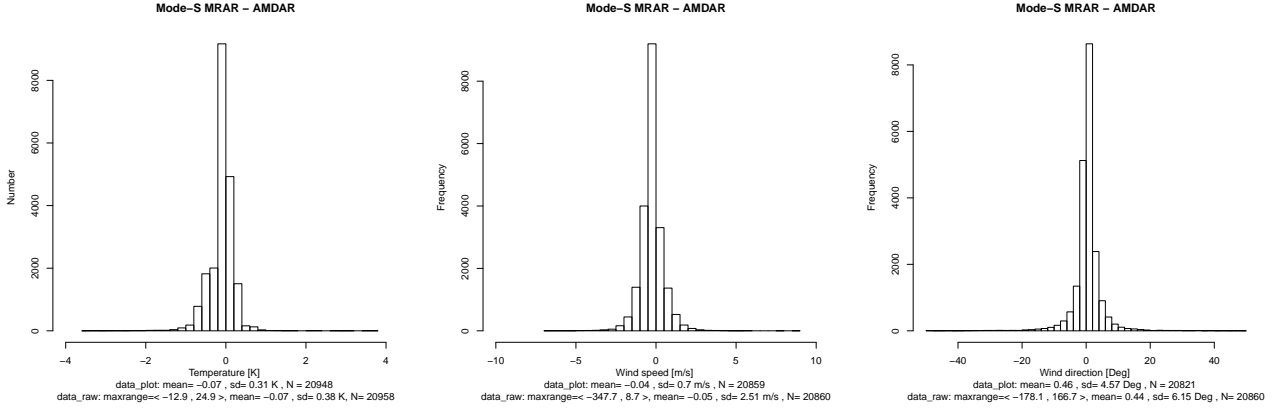
Figure 4: Histograms of Mode-S MRAR differences with respect to AMDAR for temperature (left), wind speed (middle) and wind direction (right). Only the displayed value range was used to compute histograms and extreme values are indicated below the plots.

The same gross error check (differences larger than 4 K, 10 m/s and 50° were excluded) was applied to the differences between AMDAR and Mode-S EHS. The error check reduced the data sample by around 1.6% of temperature and around 4% of wind speed collocations. The Mode-S EHS differences of the temperature and wind direction are mostly normally distributed, see Figure 5. But the distribution of wind speed differences shows a two peak distribution. The spread of the Mode-S EHS - AMDAR differences is much larger than the spread of the Mode-S MRAR - AMDAR differences, for both wind and temperature.
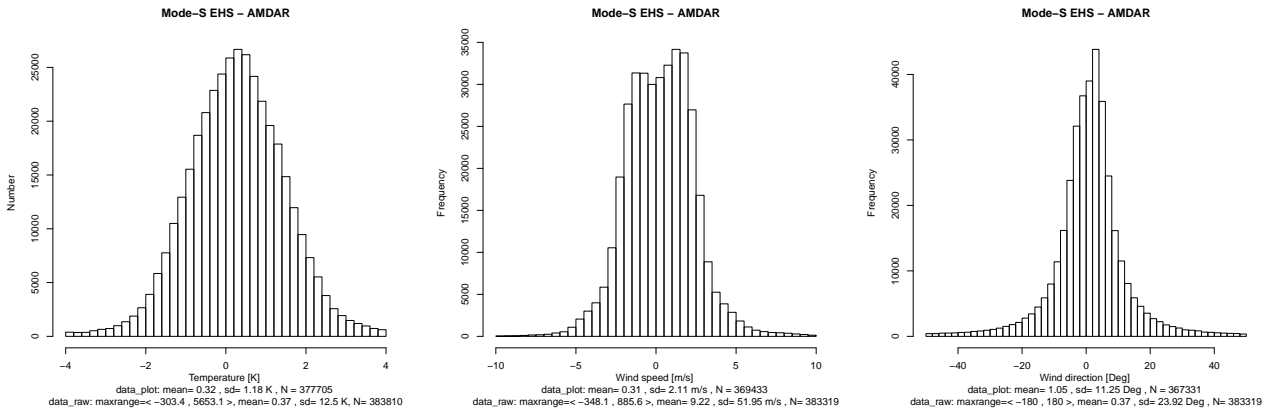
Figure 5: Histograms of Mode-S EHS differences with respect to AMDAR for temperature (left), wind speed (middle) and wind direction (right). Only the displayed value range was used to compute histograms and extreme values are indicated below the plots.

Difference statistics aggregated in one kilometer layers are shown in Figure 6. For most of Mode-S MRAR collocations there is almost no temperature bias (it ranges from around 0.01 K to -0.1 K) and only a small number below 1 km have a negative bias of -0.6 K. The root mean square (RMS) below 1 km is around 1.5 K and above it ranges from 0.6 K to 0.2 K. The Mode-S EHS collocations above 1 km are more biased (around 0.3 K). Although the temperature RMS slightly decreases with height,

it is 3–5 times larger than MRAR RMS. Mode-S MRAR wind speed and wind direction collocation biases are also minimal (it ranges from -0.06 to 0.05 m/s and from 0.1 to 0.6°) and the RMS is around 0.7 m/s and 0.5°, only small number of winds below 1 km have larger positive bias and RMS. The Mode-S EHS wind speed collocations are mostly positively biased and the RMS is again 3–5 times larger than MRAR RMS.

Reasons of the large increase of the collocations statistics below 1 km are not yet clear. Considering that especially of Mode-S MRAR statistics above 1 km are very small, measurements close to ground are not expected to be worse. But height assignment and/or preprocessing of AMDAR data is suspected to be an issue due to the higher atmospheric variability close to ground.

(a) Temperature   **(b)** Wind speed   **(c)** Wind direction
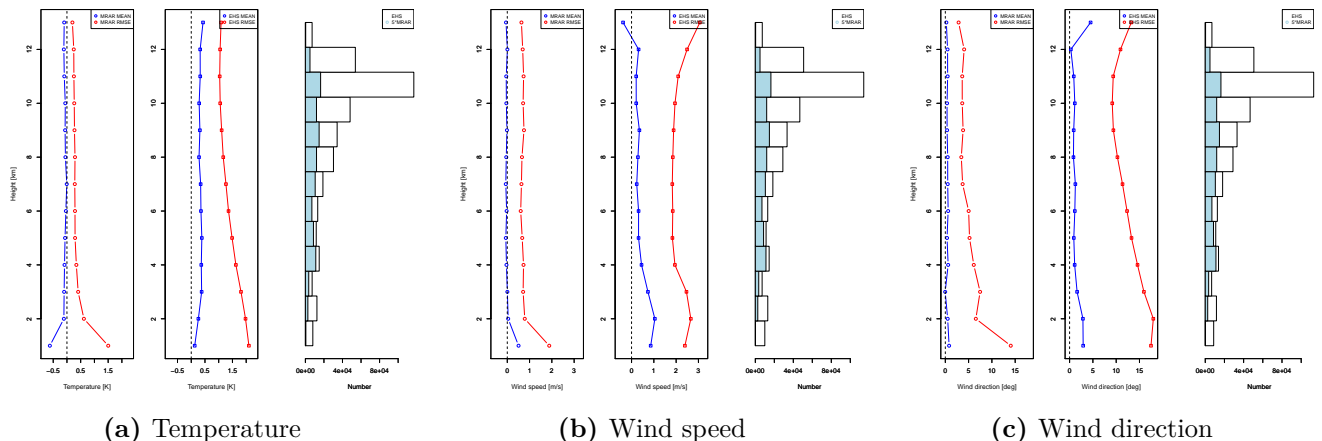
Figure 6: Vertical profile of Mode-S differences with respect to AMDAR. BIAS (blue) and RMSE (red) are displayed for each variable of MRAR (left) and EHS (middle) collocations with corresponding number of data (right).

It is important to keep in mind that not all aircraft are equipped with AMDAR and the most frequent Mode-S collocated aircraft types are listed in Table 5. Almost all (over 99%) Mode-S MRAR - AMDAR differences come from Canadair CRJ aircraft and over 95% of Mode-S EHS collocations come from Airbus A321, A320, A319, Canadair CRJ and Boeing 737. The two peak distribution of the wind speed differences is linked to the aircraft type, see distribution per aircraft type in Figure 7, but further investigation is needed to clarify the origin of errors in input parameters for Mode-S EHS wind speed computations (ground speed, air speed and magnetic heading).

Aircraft type	Number of Mode-S EHS collocations	Number of Mode-S MRAR collocations
Airbus A321	120977 (31.5%)	0
Airbus A319	101357 (26.4%)	0
Airbus A320	93424 (24.4%)	0
Canadair CRJ	28759 (7.5%)	20849 (99.9%)
Boeing 737	17972 (4.7%)	0

Table 5: Number of Mode-S - AMDAR collocations for the most frequent aircraft types.

The RMS of Mode-S MRAR - AMDAR differences are comparable with estimated uncertainty of AMDAR measurements, which means that the quality of Mode-S MRAR data is similar to AMDAR. The Mode-S EHS are slightly more biased and the RMS is around 4 times larger. The latter results are in line with the findings of de Haan (2011) who proposed more advanced preprocessing to improve the quality of Mode-S EHS data.
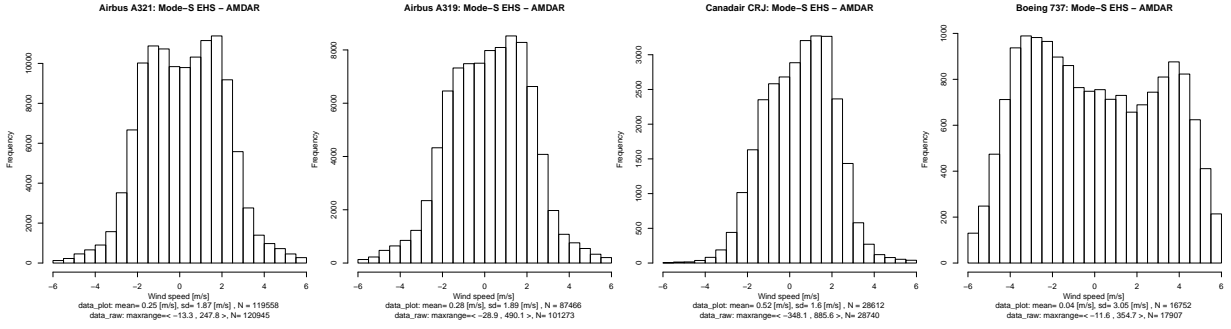
Figure 7: Distribution of Mode-EHS and AMDAR collocations for various aircraft types.

1.3.2 Mode-S validation with respect to NWP

AMDAR offers a good observation reference but is limited to AMDAR-equipped aircraft. An evaluation of all Mode-S data is possible by a comparison with NWP model, which allows sufficiently large samples for each single aircraft. However, such a comparison is limited by forecast and model errors.

The validation was performed for the Mode-S MRAR data only. The ALADIN/CHMI, detailed in the section 1.1, is used as reference. During the examined period of 1 July – 20 October 2015 around 9 million Mode-S MRAR observations were collocated with the NWP model. Operational ALADIN/CHMI forecast of various lengths (6–11 hours) were used to cover whole day with the most recent model forecast. Analyses were avoided because AMDAR observations are assimilated in the operational ALADIN/CHMI, which might limit a fair comparison. We assume that the method is robust with respect to a slight decrease of the quality with forecast ranges (between 6 and 11 hours). The assimilation configuration of the ALADIN model was used to obtain observation model equivalents to compute observation and model departures.

Only statistically reasonable aircraft sample with more than 3000 collocations are passed to data quality check. This statistical pre-selection reduced sample of data by 5% and number of aricraft by 50%. A good quality observations were selected based on criteria (mean and standard deviation of observation and model departures) partly following Strajnar *et al.* (2015), see Table 6.

	number of obs	mean	std
Temperature	3000	<1 K	<2 K
Wind speed	3000	<1 m/s	<5 m/s
Wind direction	3000	<10°	<100°

Table 6: Criteria used to generate MRAR white list of aircraft with reliable observations.

	Temperature		Wind	
	N_{data}	$N_{aircraft}$	N_{data}	$N_{aircraft}$
Total	9139677	846	9139677	846
After statistical check (n=3000)	8541019 (94%)	409	8686561 (95%)	410
After quality check	7020445 (77%)	272	7328643 (80%)	281

Table 7: Number of Mode-S MRAR - NWP collocations from 1 July – 20 October 2015.

Figure 8 shows distributions of Mode-S MRAR differences with respect to the NWP model before and after applying the quality criteria. The raw wind differences are mostly normally distributed, while temperatures are rather positively biased. The differences after quality check do not have any
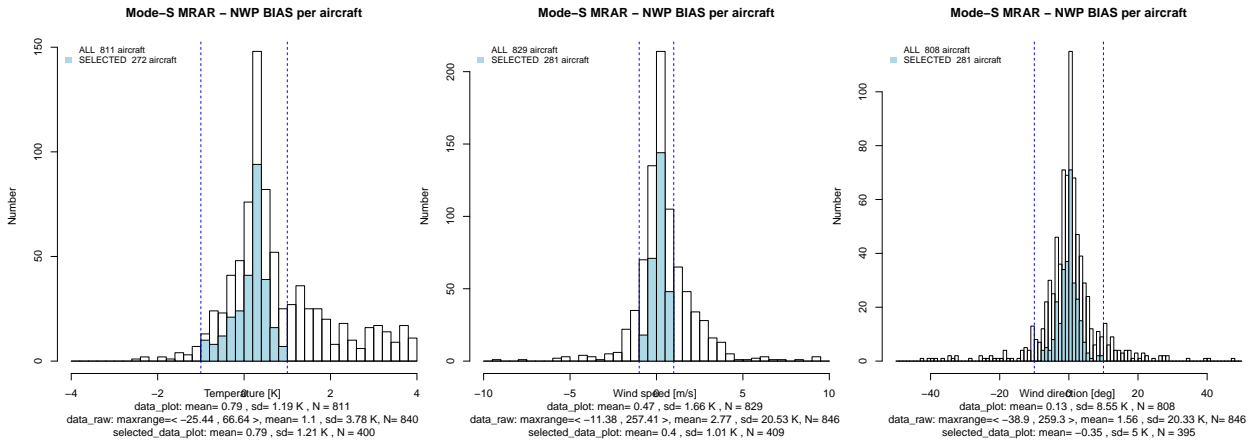
Figure 8: Histograms of Mode-S MRAR differences with respect to the NWP model ALADIN/CHMI for temperature (left), wind speed (middle) and wind direction (right). The differences after quality check are in blue. Only the displayed value range was used to compute histograms and extreme values are indicated below the plots.

(a) Temperature   **(b)** Wind speed   **(c)** Wind direction
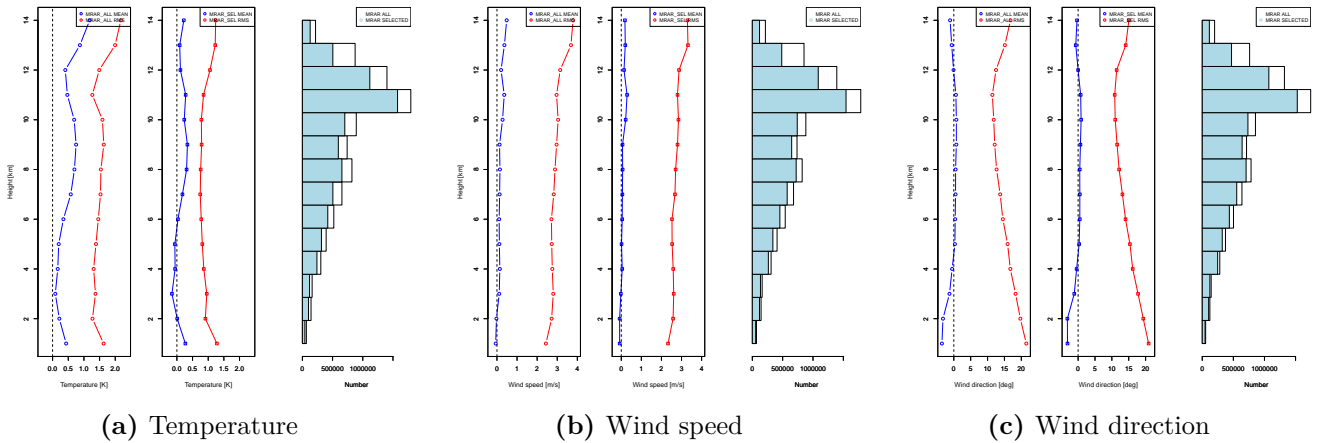
Figure 9: Vertical profiles of Mode-S MRAR differences with respect to the NWP model ALADIN/CHMI. BIAS (blue) and RMSE (red) are displayed for each variable before (left) and after the quality check (middle) with corresponding number of data (right).

systematic error, which is essential for the data assimilation. The differences were aggregated in one kilometer layers, see Figure 9. The temperature bias mostly increases with height and it is reduced by the quality check. Wind speed observation have almost no bias and the RMS is around 2.5 m/s and 3.5 m/s. Wind direction has only small bias of a few degrees below 3 km and the RMS ranges between 12 and 25°.

The quality analysis of Modes-S MRAR observations was prepared separately for temperature and wind. Approximately 77% of temperature observations from 271 aircraft (30% of the total number of aircraft) and 80% of wind observations from 281 aircraft (33% of the total number of aircraft) fulfiled required criteria, see Table 7. Finally the intersection of accepted aircraft for temperatures and winds was found to create a white list of 203 aircraft with reliable observations to be used in data assimilation experiments.

11

1.4 Assimilation impact study of Mode-S MRAR data

Only Mode-S MRAR observations are used in our first assimilation impact studies. For better readability Mode-S MRAR will be referred as MRAR in this section. The impact of MRAR observations in the NWP system ALADIN/CHMI is investigated by running two experiments. A reference experiment (REF) with the operational ALADIN/CHMI settings, detailed in the section 1.1, and a sensitivity experiment (EXP) with MRAR data added on a top of all observations assimilated in REF (i.e. SYNOP, TEMP, AMDAR, AMV and SEVIRI). For the first approximation both experiments are based on the 6-hour assimilation cycle only and production forecast for +54 hours is omitted. There are a few motivations for such experimental design. The impact of Mode-S observations is expected mainly for the first hours of a forecast (De Haan and Stoffelen, 2012) and hence the 6-hour forecast in the assimilation cycle is sufficient for the first study. Furthermore, experiments without productions are less time and computationally consuming.

1.4.1 Verification methodology

The MRAR data are very high resolution and local, covering only the Czech Republic and its near surroundings. To verify the impact of MRAR on forecast, an appropriate observational reference is needed. In order to properly address the impact of MRAR observations, verification is limited to a sub-area of the model domain covered by Mode-S observations displayed in Figure 10 (right). The sub-domain is well-covered by AMDAR and MRAR observations at the upper levels, whereas there are limited TEMP observations available at 00, 12 UTC (12 stations) and even less at 06 and 18 UTC (5 stations). Despite the sparse coverage, all observations AMDAR, TEMP and MRAR are used for the verification. In case of the comparison with MRAR themselves the interpretation of the verification scores should be aware of altitude-dependent density of MRAR (Strajnar *et al.*, 2015) with good domain coverage at higher levels and local coverage (around airports) at low altitudes. As for TEMP observations the interpretation of the verification results should be aware of the sparse coverage at 06 and 18 UTC, which can affect the average statistics at particular levels and ranges.
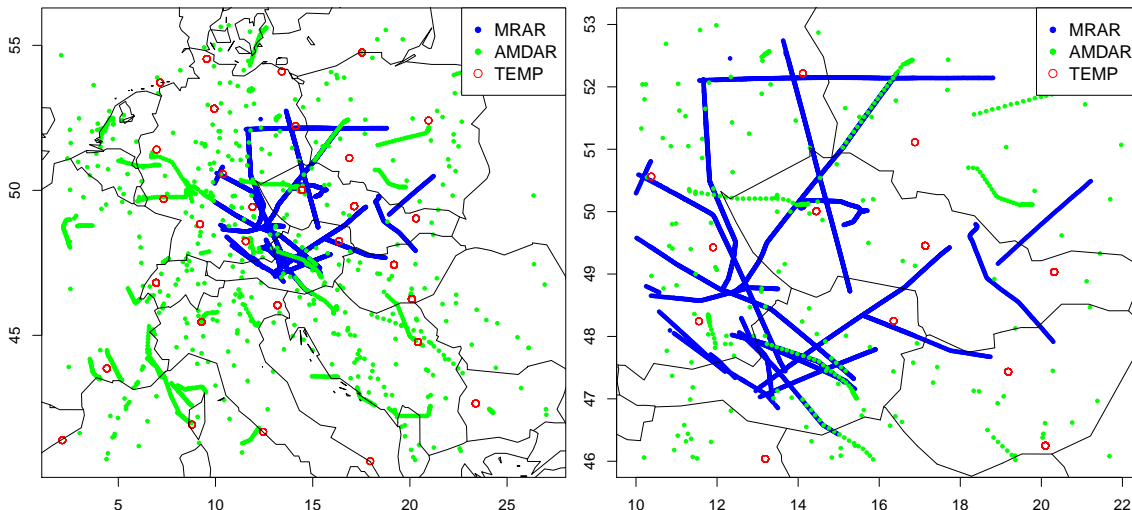
Figure 10: Horizontal coverage of MRAR (blue), AMDAR (green) and TEMP (red) observations at 12 UTC for 18 July 2015 (left). The sub-area used for verifications (right).

For verification purpose, the MRAR and AMDAR observations ±30 minutes around each hour are used. The verification sample of MRAR observation includes the subset of independent observations not assimilated in analysis time. Three main statistical scores are computed using departures of forecasted parameters $H(x^f)_i$ at the observation points and actual measured values y_i:

- mean absolute error $MAE = \frac{1}{n} \sum_{i=1}^{N} (|H(x^f)_i - y_i|)$

- root mean square error $RMSE = \sqrt{\sum_{i=1}^{N} \frac{1}{N}(H(x^f)_i - y_i)^2}$

- standard deviation $STDE = \sqrt{(RMSE^2 - MAE^2)}$

1.4.2 Impact of MRAR observations on assimilation cycle

Impact of MRAR observations on assimilation cycle was evaluated for the period 1 June – 30 June 2015. The hourly temperature and wind forecast up to +6 h from 00, 06, 12 and 18 UTC were compared with AMDAR, TEMP and MRAR observations.

Comparison with AMDAR and TEMP observations
Figure 11 shows the statistics of the model forecast against AMDAR (columns 1–2) and TEMP (columns 3–4) observations for the experiments REF and EXP at the levels (400 hPa and 700 hPa). In both comparisons, the experiment EXP using MRAR observation shows an increase of RMSE and MAE at analysis time when compared to the experiment REF. This detrimental effect is because of AMDAR and TEMP observations are already assimilated in the reference experiment and the same data are also used for the verifications. In case of AMDAR verification, this effect is propagated to the first hour of forecast when we assimilate both AMDAR and MRAR data within the ±90 minutes assimilation window.
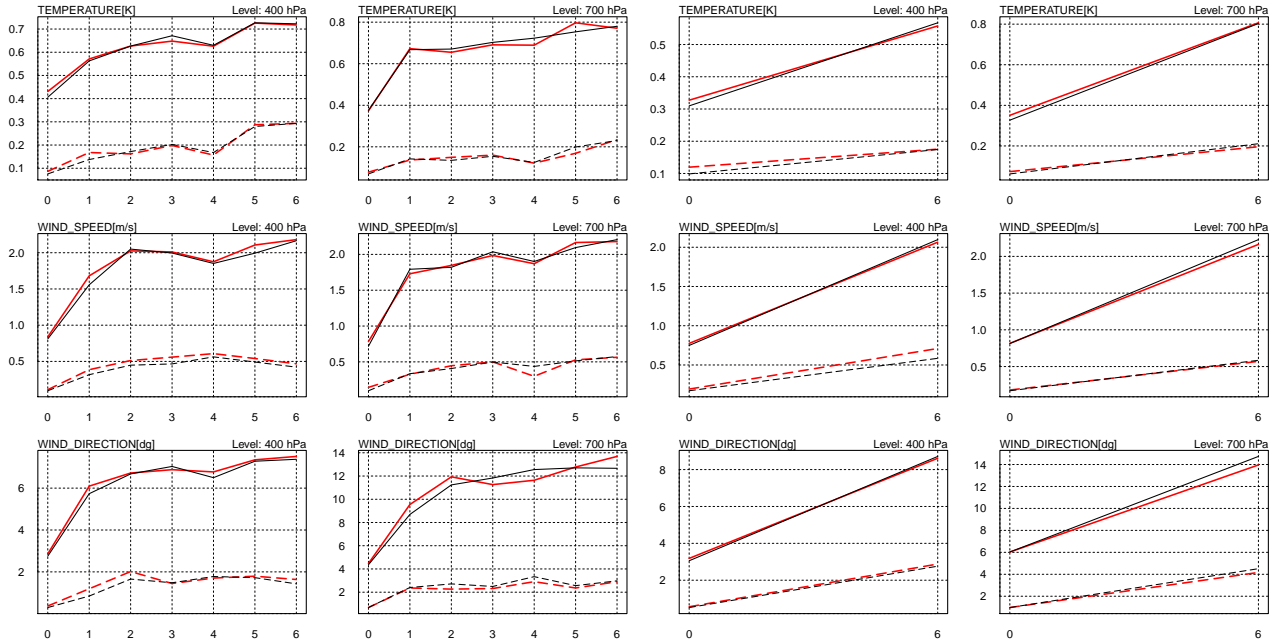
Figure 11: Statistics for the comparison of the model forecast against AMDAR (columns 1–2) and TEMP (columns 3–4) observations for experiments REF (black) and EXP (red) at 400 hPa and 700 hPa. The MEA (dash lines) and RMSE (solid lines) are plotted for (top to bottom) temperature, wind speed and wind direction.

For both AMDAR and TEMP verifications we observed almost neutral impact on RMSE for all parameters in the next 2–6 hours of forecast. Only a small degradation of MAE for the wind speed at the higher levels (300 hPa and 400 hPa) and the small positive impact of assimilating MRAR data on the MAE of the wind direction at the 700 hPa level were detected.

Comparison with Mode-S MRAR observations

Figure 12 shows the statistics of the model forecast against MRAR observations for both experiments at the same levels (400 hPa and 700 hPa). Obviously at analysis time, experiment EXP using MRAR observation show the lowest RMSE and MAE when compared to MRAR. At higher levels a positive impact of assimilating MRAR is observed for RMSE and MAE, however this impact disappear after few hours (1–2 h). The duration of the positive impact differs for different levels and parameters. A slight positive impact on RMSE is observed up to 3 hours for temperature as well as up to 6 hours of forecast for both wind parameters.
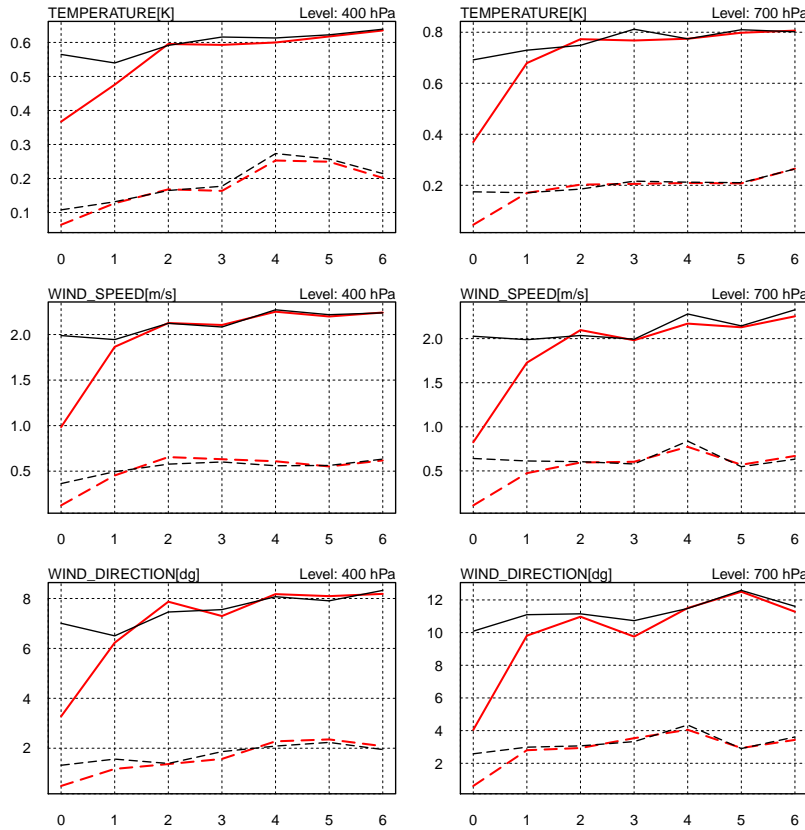
Figure 12: Statistics for the comparison of the model forecast against Mode-S MRAR observations for experiments REF (black) and EXP (red) at 400 hPa (left) and 700 hPa (right). The MEA (dash lines) and RMSE (solid lines) are plotted for (top to bottom) temperature, wind speed and wind direction.

Overall, the results indicate that MRAR data assimilation has a positive impact on the wind at the lower levels, while at the higher levels, there is a neutral impact on all parameters in RMSE and the MAE degradation of the wind speed. The negative effect is probably due to overfitting of the MRAR observations in analysis and can be enhanced by spreading the MRAR information outside their location due to the simplified background error covariance structures. The preliminary results are encouraging and an optimization of MRAR data assimilation, e.g. tuning of the observation weights, will be a subject of the further investigation.

1.5 Diagnostic analyses

The goal of diagnostic analyses is to produce atmospheric state as close as possible to reality taking into account all available information, such as observed data, the NWP model, physical constrains and climatology. Diagnostic analyses aim to provide an up-to-date three dimensional state of the atmosphere in chosen grid as soon as possible. They can be seen as nowcasting for period of 0 hour.
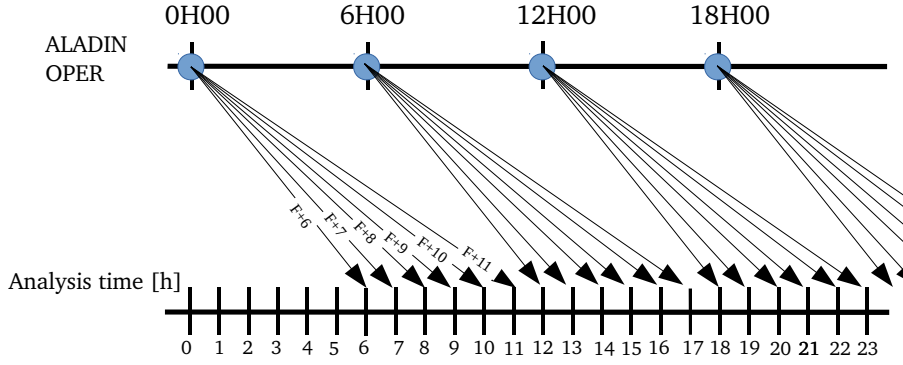
Figure 13: The diagnostic analyses are using as first guess the operational forecast of the ALADIN/CHMI model for different lead times, this is denoted by F+n hour forecast in the figure.

Diagnostic analyses help to identify regions where severe weather events, such as wind sheer, turbulence or convection, could appear. Detection of such regions is very important for the safety of air traffic. Furthermore, a comparison of diagnostic analyses with issued weather forecast gives a feedback to forecast quality.

The interpolation of available observations is not sufficient for a comprehensive description of the current atmospheric state. Moreover, many observations are not available in near real time, but with a considerable delay. We propose a combination of observations with the first guess given by the operational NWP model ALADIN/CHMI to provide diagnostic analyses. Atmospheric fields are analyzed using the 3D-Var method and near-surface parameters by OI method. An automatic system to produce such diagnostic analyses was designed. The system settings and the first results follows.

1.5.1 Setup

The quality of diagnostic analyses rely upon input data and used methodology. ALADIN/CHMI operational forecasts with different lead times are used as the first guess, see Figure 13, to exploit the latest model outputs.

A baseline setup of the 3D-Var and OI methods relies on the BlendVar configuration operational at CHMI, described in the section 1.1. The first difference is the order of the 3D-Var and OI method, which is swapped. Initialization of soil variables is assumed to be less important for the diagnostic analyses and it is suppressed. In that case analysis of upper-air variables is done first. The OI method is employed afterwards to analyze screen-level parameters, such as 2 m temperature and relative humidity and 10 m wind speed and wind direction. This concept is not used in the operational framework because the above mentioned screen-level parameters are diagnosed and can not be incorporated into the subsequent model forecast. The setup of OI method is tuned to consider only surface stations up to altitude of 1500 m. The observations where the difference between the model orography and the station altitude is larger than 800 m are not assimilated. The horizontal correlation length-scale are decreased in the OI analysis to make it more local.

Similarly, the 3D-Var method can be further tuned to fit the observation closer. Following Auger and Teseva (2004) the model standard deviation error decrease can be beneficial. Reformulation of the background error covariance matrix generated by local ensemble of assimilation with perturbed observations (Berre *et al.*, 2006) will be investigated.

The number of available observations is varying during time of a day. The observation processing starts with a delay to collect as much observations as possible to constrain the analysis. The delay of 20 minutes seems to be a reasonable compromise between the number of available observations and the time of the diagnostic analysis availability, e.g. approximately 30 minutes after its validity time.
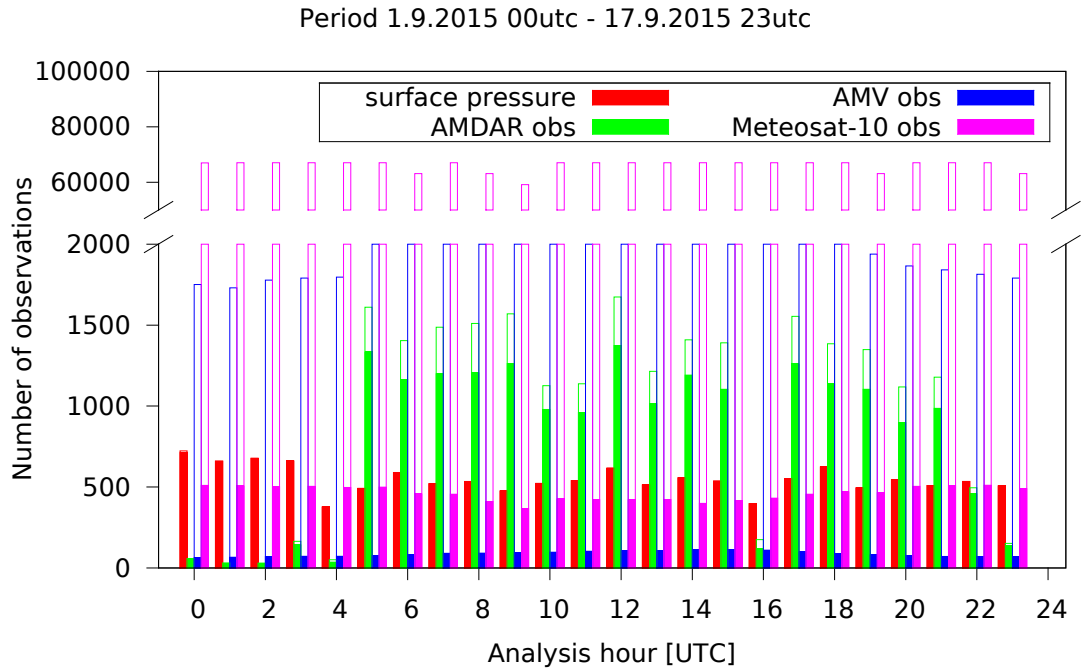
Figure 14: The average number of available observations at analysis start (empty boxes) and the average number of used observations in the upper-air analysis (filled boxes).

Near-surface observations are collected from synoptic and automatic stations. Around 3700 near-surface observations are assimilated by OI method. These observations comprise surface pressure, 2 m temperature and relative humidity, 10 m wind speed and wind direction. However, only surface pressure from near-surface observations is used in the upper-air analysis. Aerological soundings are important source of upper-air information. Unfortunately they are available only 2–4 times a day at 00, 06, 12, 18 UTC and they come too late to be used in diagnostic analysis. Approximately 500 radiances from Meteosat-10 and only a few atmospheric motion vectors (AMV) are assimilated in the upper-air analysis. For every analysis in the daytime (05–21 UTC) there are around 1400 aircraft observations from AMDAR reports available, while at night (22–04 UTC) their number is very low. Figure 14 shows average number of available observations at analysis start and assimilated observations for each analysis. Overall about 2500 observations are assimilated in the upper-air analysis in the daytime. Around half of used observation comes from aircraft and this number will be further increased by MRAR observations. It is expected that the total number of assimilated observations will be increased by Mode-S MRAR data by half.

1.5.2 First results

A temperature inversion was observed over Prague on 3 December 2015 at 06 UTC. Aerological sounding is not available when analysis production starts and sounding data are used as reference. The first guess captured the inversion already quite well, see Figure 15. Only other source of vertically dense observations are aircraft measurements. Whereas the reference analysis already assimilating AMDAR observations did not improve description of the inversion (blue line), the analysis assimilating MRAR observations (green line) is much closer to the aerological sounding (black line) and MRAR observations (light blue crosses).

The first impact study is promising and shows better description of temperature inversion thanks to MRAR data assimilation. The prototype of hourly diagnostic analyses production is prepared. The analysis scheme is based on 3D-Var and OI methods of ALADIN/CHMI system and like this it can
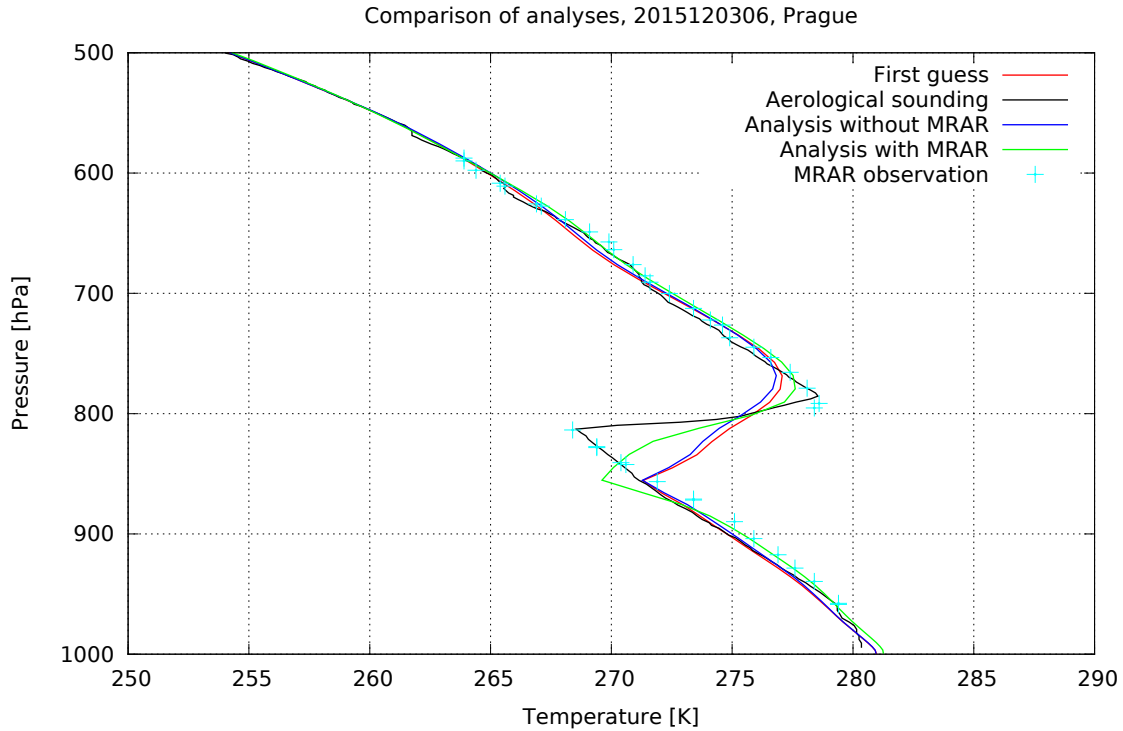
Figure 15: The comparison of analysis with and without MRAR observations and corresponding observations.

assimilate conventional observations, including MRAR data and satellite radiances. Moreover, it is ready to assimilate other remote sensing observations, such as Doppler winds and reflectivity from ground-based radars and ground-based GPS measurements. The prototype can be further improved to comply with the nowcasting spirit of the diagnostic analyses, e.g. fit to observations can be further increased and the background error covariances can be tuned.

1.6 Summary

Aircraft-based observations are beneficial for the aviation community, NWP regional modeling and nowcasting applications. New Mode-S observations available via the modern air traffic surveillance systems were investigated.

The quality of Mode-S temperature and wind observations available in the airspace of the Czech Republic was assessed. The collocation with AMDAR observations revealed that Mode-S EHS observations have larger variability and errors. Mode-S MRAR observations are of comparable quality to AMDAR and they are suitable for data assimilation simply after the quality check based on the statistics of differences with respect to the NWP model.

The state-of-the-art NWP system ALADIN/CHMI was used to evaluate impact of new aircraft Mode-S MRAR observations on forecast. An appropriate observational reference for verification is questionable considering very high resolution of MRAR data in time and space. Verification against soundings and AMDAR aircraft observations showed mostly neutral impact, slight degradation was found at higher levels, while slight positive impact was observed at lower levels for wind. Verification against independent Mode-S MRAR observations, which are considered as suitable high resolution reference, showed clear positive impacts in the first forecast hours.

Use of Mode-S MRAR observations was explored to improve a near real time high resolution diagnostic analysis with promising results. Such analyses aim to provide self-consistent diagnostic of the atmosphere using all available observation and the NWP model as soon as possible. Key

issue is a fast provision and processing of all available observation to constrain the analysis. The prototype of hourly diagnostic analyses production was prepared. The system relies on the NWP model ALADIN/CHMI and it can assimilate Mode-S MRAR observation and also other conventional and remote sensing observations.

Newly developed methods to derive aircraft observations seems to be a promising extension of aircraft observation coverage over Europe. The observations have a potential to improve the first hours of NWP forecast. They are also beneficial for the aviation community for current and future air traffic management concepts, both as observations and via improved and more accurate weather forecast.

Acknowledgments

References

Auger L, Teseva L. 2004. VARPACK – A diagnostic Tool , based on the 3DVar/ALADIN surface scheme. Technical Report 1, Météo-France, URL `http://www.cnrm.meteo.fr/aladin-old/newsletters/news27/ArtAUGER.pdf`.

Benjamin SG, Schwartz BE, Cole RE. 1999. Accuracy of ACARS wind and temperature observations determined by collocation. *Weather and Forecasting* **14**(6): 1032–1038.

Berre L. 2000. Estimation of synoptic and mesoscale forecast error covariances in a limited-area model. *Monthly Weather Review* **128**(3): 644–667.

Berre L, Stefanescu SE, Pereira MB. 2006. The representation of the analysis effect in three error simulation techniques. *Tellus A* **58**(2): 196–209, doi:10.3402/tellusa.v58i2.14761, URL `http://tellusa.net/index.php/tellusa/article/view/14761`.

Brožková R, Klaric D, Ivatek-Šahdan S, Geleyn JF, Cassé V, Široká M, Radnoti G, Janoušek M, Seidl H. 2001. DFI blending: An alternative tool for preparation of the initial conditions for LAM. *Research activities in atmospheric and oceanic modelling, WMO CAS/JSC WGNE Rep.* **31**.

Courtier P, Thépaut JN, Hollingsworth A. 1994. A strategy for operational implementation of 4D-Var, using an incremental approach. *Quarterly Journal of the Royal Meteorological Society* **120**(519): 1367–1387.

de Haan S. 2011. High-resolution wind and temperature observations from aircraft tracked by Mode-S air traffic control radar. *Journal of Geophysical Research: Atmospheres (1984–2012)* **116**(D10).

De Haan S, Stoffelen A. 2012. Assimilation of high-resolution Mode-S wind and temperature observations in a regional NWP model for nowcasting applications. *Weather and Forecasting* **27**(4): 918–937.

Giard D, Bazile E. 2000. Implementation of a new assimilation scheme for soil and surface variables in a global NWP model. *Monthly Weather Review* **128**(4): 997–1015.

Noilhan J, Planton S. 1989. A simple parameterization of land surface processes for meteorological models. *Monthly Weather Review* **117**(3): 536–549.

Painting JD. 2003. AMDAR reference manual. Technical report, WMO-no.958 *available online*, URL `https://www.wmo.int/pages/prog/www/GOS/ABO/AMDAR/publications/AMDAR_Reference_Manual_2003.pdf`. 84 pp.

Schwartz B, Benjamin SG. 1995. A comparison of temperature and wind measurements from ACARS-equipped aircraft and rawinsondes. *Weather and forecasting* **10**(3): 528–544.

Strajnar B. 2012. Validation of Mode-S Meteorological Routine Air Report aircraft observations. *Journal of Geophysical Research: Atmospheres (1984–2012)* **117**(D23).

Strajnar B, Žagar N, Berre L. 2015. Impact of new aircraft observations Mode-S MRAR in a mesoscale NWP model. *Journal of Geophysical Research: Atmospheres* **120**(9): 3920–3938, doi: 10.1002/2014JD022654, URL `http://dx.doi.org/10.1002/2014JD022654`. 2014JD022654.

WMO. 2014a. Requirements for the Implementation and Operation of an AMDAR Programme. Technical report, WIGOS-no.2014-02. 31 pp.

WMO. 2014b. The Benefits of AMDAR Data to Meteorology and Aviation. Technical report, WIGOS-no.2014-01. 50 pp.